

Characteristics of Bay of Bengal monsoon depressions in the 21st Century

Article

Published Version

Rastogi, D., Ashfaq, M., Leung, L. R., Ghosh, S., Saha, A., Hodges, K. ORCID: <https://orcid.org/0000-0003-0894-229X> and Evans, K. (2018) Characteristics of Bay of Bengal monsoon depressions in the 21st Century. *Geophysical Research Letters*, 45 (13). pp. 6637-6645. ISSN 0094-8276 doi: <https://doi.org/10.1029/2018GL078756> Available at <https://centaur.reading.ac.uk/78092/>

It is advisable to refer to the publisher's version if you intend to cite from the work. See [Guidance on citing](#).

To link to this article DOI: <http://dx.doi.org/10.1029/2018GL078756>

Publisher: American Geophysical Union

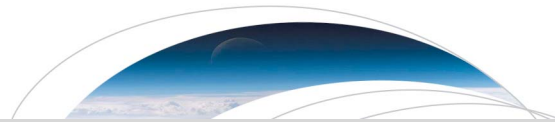
All outputs in CentAUR are protected by Intellectual Property Rights law, including copyright law. Copyright and IPR is retained by the creators or other copyright holders. Terms and conditions for use of this material are defined in the [End User Agreement](#).

www.reading.ac.uk/centaur

CentAUR

Central Archive at the University of Reading

Reading's research outputs online



Geophysical Research Letters

RESEARCH LETTER

10.1029/2018GL078756

Key Points:

- Increase in radiative forcing does not significantly impact the frequency of South Asian summer monsoon depressions in the GCMs
- Climatological frequency of MDs depends on the strength of the background dynamic and thermodynamic conditions
- Changes in the extreme wet events are dominated by nondepression day occurrences, rendering future monsoon extremes less predictable

Supporting Information:

- Supporting Information S1
- Data Set S1

Correspondence to:

M. Ashfaq,
mashfaq@ornl.gov

Citation:

Rastogi, D., Ashfaq, M., Leung, L. R., Ghosh, S., Saha, A., Hodges, K., & Evans, K. (2018). Characteristics of Bay of Bengal monsoon depressions in the 21st century. *Geophysical Research Letters*, 45. <https://doi.org/10.1029/2018GL078756>

Received 15 MAY 2018

Accepted 14 JUN 2018

Accepted article online 21 JUN 2018

©2018. American Geophysical Union.
All Rights Reserved.

This manuscript has been authored by UT-Battelle, LLC, under contract DE-AC05-00OR22725 with the US Department of Energy (DOE). The US government retains and the publisher, by accepting the article for publication, acknowledges that the US government retains a nonexclusive, paid-up, irrevocable, worldwide license to publish or reproduce the published form of this manuscript, or allow others to do so, for US government purposes. DOE will provide public access to these results of federally sponsored research in accordance with the DOE Public Access Plan (<http://energy.gov/downloads/doe-publicaccess-plan>).

Characteristics of Bay of Bengal Monsoon Depressions in the 21st Century

Deeksha Rastogi¹ , Moetasim Ashfaq¹ , L. Ruby Leung² , Subimal Ghosh³ , Anamitra Saha³, Kevin Hodges⁴, and Katherine Evans¹ 

¹Computational Science and Engineering Division, Oak Ridge National Laboratory, Oak Ridge, TN, USA, ²Atmospheric Sciences and Global Change Division, Pacific Northwest National Laboratory, Richland, WA, USA, ³Department of Civil Engineering, Indian Institute of Technology Bombay, Mumbai, India, ⁴Department of Meteorology, University of Reading, Reading, UK

Abstract We show that 21st century increase in radiative forcing does not significantly impact the frequency of South Asian summer monsoon depressions (MDs) or their trajectories in the Coupled Model Intercomparison Project Phase 5 general circulation models (GCMs). A significant relationship exists between the climatological occurrences of MDs and the strength of the background upper (lower) tropospheric meridional (zonal) winds and tropospheric moisture in the core genesis region of MDs. Likewise, there is a strong relationship between the strength of the meridional tropospheric temperature gradient in the GCMs and the trajectories of MDs over land. While monsoon dynamics progressively weakens in the future, atmospheric moisture exhibits a strong increase, limiting the impact of changes in dynamics on the frequency of MDs. Moreover, the weakening of meridional tropospheric temperature gradient in the future is substantially weaker than its inherent underestimation in the GCMs. Our results also indicate that future increases in the extreme wet events are dominated by nondepression day occurrences, which may render the monsoon extremes less predictable in the future.

Plain Language Summary Monsoon depressions (MDs) are one of the most important synoptic scale transient weather systems that transport large amount of moisture over the South Asian landmass and contribute significantly to the total precipitation. In this study, we investigate representation of MDs in the Coupled Model Intercomparison Project Phase 5 general circulation models, their simulated responses to increase in radiative forcing during the 21st century under Representative Concentration Pathway 8.5, and the resulting changes in precipitation characteristics at intraseasonal time scales. We show that 21st century increase in radiative forcing does not significantly impact the frequency of South Asian summer monsoon depressions or their trajectories in the general circulation models. Our results indicate a significant relationship between the climatological occurrences of MDs and the background upper (lower) tropospheric meridional (zonal) winds and tropospheric moisture in the core genesis region of MDs. While monsoon dynamics progressively weakens in the future, atmospheric moisture exhibits a strong increase, limiting the impact of changes in dynamics on the frequency of MDs. Our results also indicate that future increase in the extreme wet events is dominated by nondepression day extremes, which may render the monsoon extremes less predictable in the future.

1. Introduction

Monsoon depressions (MDs) are one of the most important synoptic scale transient weather systems that transport large amounts of moisture over the South Asian landmass and contribute significantly to the total precipitation over major parts of South Asia during the summer season (June-July-August-September; JJAS; Sikka, 1977). Most of the MDs originate over the Bay of Bengal (BoB) and propagate west northwestward along the monsoon trough with a lifespan of 2 to 7 days and often contribute to severe flooding, widespread property damage, and loss of life. For instance, the July 2010 flooding in Pakistan (Galarneau et al., 2012) and June 2013 flooding in Uttarakhand, India (Singh et al., 2014), were the result of prolonged periods of intense rainfall during the lifecycle of MDs, with a combined total of over \$10 billion in economic losses and over 5,000 deaths (Sharjeel et al., 2012). Long-term records indicate that there is genesis of five or more MDs over the BoB on average during a summer season, but there has been a controversy regarding the trends in their yearly frequency in recent decades. Several observational studies, based on the records of the Indian Meteorological Department archives, indicate a decreasing trend in MDs over the last 40 years, related to

the anomalies in the monsoon dynamics (e.g., weakening of the upper troposphere tropical easterly jet; Dash et al., 2004; Rao et al., 2004) and/or in the thermodynamics (e.g., a decrease in midtroposphere relative humidity; Prajeesh et al., 2013; Vishnu et al., 2016). However, a recent study questioned the accuracy of the Indian Meteorological Department MD archives and the associated decreasing trends (Cohen & Boos, 2014). On the other hand, future projections of monsoon dynamics and summer precipitation indicate an increasingly moisture-driven monsoonal response to increasing radiative forcing with most GCMs simulating wetter summers over South Asia despite a weakening of the monsoon dynamics (Annamalai et al., 2007; Mei et al., 2015). Moreover, while GCMs are able to simulate the structure of MDs well (Hunt et al., 2016), less is known about their accuracy in the simulation of MDs frequency and trajectories over land. Within this context, the ability of GCMs to represent the fundamental characteristics of MDs and the robustness of their projected future variations in response to enhanced greenhouse gas forcing comes into question as the current generation of GCMs is shown to be lacking the desired level of skill over South Asia (Ashfaq et al., 2016; Boos & Hurley, 2013; Hagos et al., 2018; Ramesh & Goswami, 2014; Sperber et al., 2013). With this backdrop of uncertainties and the inextricable dependency of the South Asian summer monsoon precipitation on MDs, we investigate their representation in the Coupled Model Intercomparison Project Phase 5 (CMIP5) general circulation models (GCMs), their simulated responses to increases in radiative forcing during the 21st century under Representative Concentration Pathway 8.5 (RCP8.5), and the resulting changes in the precipitation characteristics at intraseasonal time scales.

2. Methods

2.1. Data Sets

We analyze the CMIP5 historical and RCP8.5 GCM experiments for 41 years (1965–2005) in the historical period and 90 years (2010–2099) in the future period. The analysis of the historical period is based on the data from 27 GCMs; however, only 20 of these GCMs have data available for the future period (Table S1 in the supporting information). For the evaluation of MDs and their environments in the historical period and to provide a comparison with the GCMs, we used zonal and meridional winds, temperature, and moisture from three Reanalysis data sets (National Centers for Environmental Prediction [NCEP]/National Center for Atmospheric Research Reanalysis I [NCEP-R1; Kistler et al., 2001], Modern-Era Retrospective analysis for Research and Applications 2 [MERRA2; Gelaro et al., 2017], and ERA-Interim [ERA-I; Dee et al., 2011]), precipitation over land from the Climate Research Unit data (Harris et al., 2014), and precipitation over ocean from the Climate Prediction Center data (Xie et al., 2003). We use NCEP R1 as the main reference, whereas MERRA2 and ERA-I comparisons are shown for the overlapping years (1981–2005) in the historical period. For consistency, we only use the vertical pressure levels that are common across all Reanalysis and GCMs.

2.2. MD Identification and Characterization

We apply a feature-tracking algorithm, detailed in Hodges (1995, 1999), to identify and track the MDs over South Asia during the JJAS monsoon period. This method has the capability to produce trajectories for cyclonic systems by identifying and tracking maxima in 850-mb relative vorticity and has been previously employed for similar investigations (Ashfaq et al., 2016; Cohen & Boos, 2014; Hurley & Boos, 2015). In order to focus on the synoptic scale disturbances, the tracking algorithm filters out the planetary spatial scales from the vorticity field for total wave numbers less than or equal to 5 and truncates it to T42 before the tracking is applied to suppress noise in the vorticity field and to perform the identification at a common spatial scale for all Reanalysis and models. Our analysis is only focused on the westward-northwestward moving BoB MDs that travel over the South Asian landmass. Among the identified low-pressure systems, we select a low-pressure system as an MD if it passes through the BoB between 10°N and 23°N, moves westward or northwestward over land, has a lifespan of more than 2 days, and travels a distance of at least 500 km. Land-only and ocean-only low-pressure systems are not considered in our analyses. All westward moving MDs data sets used in this study are part of the supplementary material (see supporting information).

We use the Central India domain (16.5°N–26.5°N and 74.5°E–86.5°E; hereafter CI domain) for the detailed analysis of the characteristics of MDs over the South Asian landmass. The CI domain is considered the most homogenous in terms of the precipitation distribution over South Asia (Goswami et al., 2006). The precipitation contribution from MDs is calculated as the domain average over the CI domain from a day before a depression enters the CI domain until the day after it leaves during JJAS. Extreme precipitation

days at each grid point are calculated as the number of days during JJAS that cross grid specific 95th percentile of annual precipitation on wet days (i.e., days with >1-mm precipitation) averaged over the historical period.

We characterize the background environment prerequisite for MD occurrences during the summer season by defining an index (hereafter MD-index) as a product of (i) specific humidity averaged over 80°E to 100°E and 10°N to 30°N and 850 to 500 mb in the vertical and (ii) the sum of the absolute values of zonal winds at 850 mb, averaged over 50°E to 80°E and 5°S to 18°N, and meridional winds at 200 mb, averaged over 80°E to 100°E and 5°S to 30°N ($[|U_{850}| + |V_{200}|] \times [Q_{850 \text{ to } 500}]$). U_{850} (westerly, positive) and V_{200} (northerly, negative) are the lower and upper tropospheric components of the regional branches of the Walker and Hadley circulations. Therefore, the magnitude of $[|U_{850}| + |V_{200}|]$ reflects the overall strength of the background dynamics. The magnitude of $Q_{850 \text{ to } 500}$ represents the amount of lower to middle tropospheric moisture in the core region of the MDs genesis, a substantial amount of which is considered necessary for deep convection in the tropics (Holloway & Neelin, 2009; Soden & Fu, 1995). The suitability of the background environment is calculated as a long-term average over the historical period and two future periods (2010 to 2054 and 2055 to 2099) for each GCM. It should be noted that the MD-index only measures the suitability of the background conditions as a prerequisite for MD genesis at long-term seasonal time scales and therefore is not capable to explain the mechanisms leading up to individual cyclogenesis. Also, given that the background environment does not change drastically at interannual time scales, the MD-index is more useful for intermodel comparison or analysis of long-term variations and may not relate well with the year-to-year variations in the frequency of MDs within a model or Reanalysis.

Additionally, we calculate the strength of the meridional tropospheric temperature gradient (hereafter MTG) as the difference of the climatological mean temperature at 30°N and 5°N, averaged over (i) the zonal belt between 50°E and 85°E and (ii) the upper tropospheric layers between 200 and 500 hPa (Ashfaq et al., 2009). The various domains used for the different analyses are shown in Figure S1 in the supporting information.

2.3. Trend Analysis

We apply several measures for the analysis of trends in the characteristics of the MDs in the future period (2010–2099) of CMIP5 GCMs. (a) Ensemble mean time series of (i) all MDs with lifespan >2 days, (ii) MDs with lifespan ≥ 5 days, and (iii) MDs with lifespan >2 and <5 days are standardized with respect to their mean and standard deviation, and a 5-year moving average filter is applied. The modified Mann-Kendall test (Hamed & Rao, 1998) is applied to each time series to determine the significance of the trends during the 2010–2099 period. (b) Each of the three time series from (a) is divided in two halves (2010–2054 and 2055–2099), and the significance of changes in the occurrence of MDs is calculated for the second half relative to the first half. A two sample *t* test is used for the statistical significance, where *p* values ≤ 0.05 are used to reject the null hypothesis. (c) Individual GCM time series of (i) all MDs with lifespan >2 days, (ii) MDs with lifespan ≥ 5 days, and (iii) MDs with lifespan >2 days and <5 days; (iv) average lifespan of MD and (v) total number of JJAS days with an MD over land (MD-days) are standardized with respect to their mean and standard deviation, and a 5-year moving average filter is applied. Two separate Poisson distributions are fitted to each half of the future period (2010–2054 and 2055–2099) time series, and the change is calculated at different levels of cumulative distribution function. (d) A linear trend corresponding to the minimum mean square error is calculated for each GCM, and the normalized trend results are represented by a boxplot. The upper and lower bound of the box represents the 25th and 75th percentile values, and the middle one represents the 50th percentile.

3. Results and Discussion

3.1. MDs in the Historical Period

Monsoon depressions exhibit several distinct characteristics related to their occurrences, trajectories, and contribution to the summer precipitation (Figure 1). During the historical period (1981–2005), 5.5 (5.4 when 1965–2005 is considered), 5.8, and 5.8 westward moving MDs per year were identified that pass through the BoB in NCEP R1, MERRA2, and ERA-I, respectively, following the criteria described in section 2. At least 90% of these follow a trajectory that takes them north of 20°N during their life span over the land of South Asia (Figure 1). It should be noted that the frequency of MDs may increase in Reanalysis data sets when both

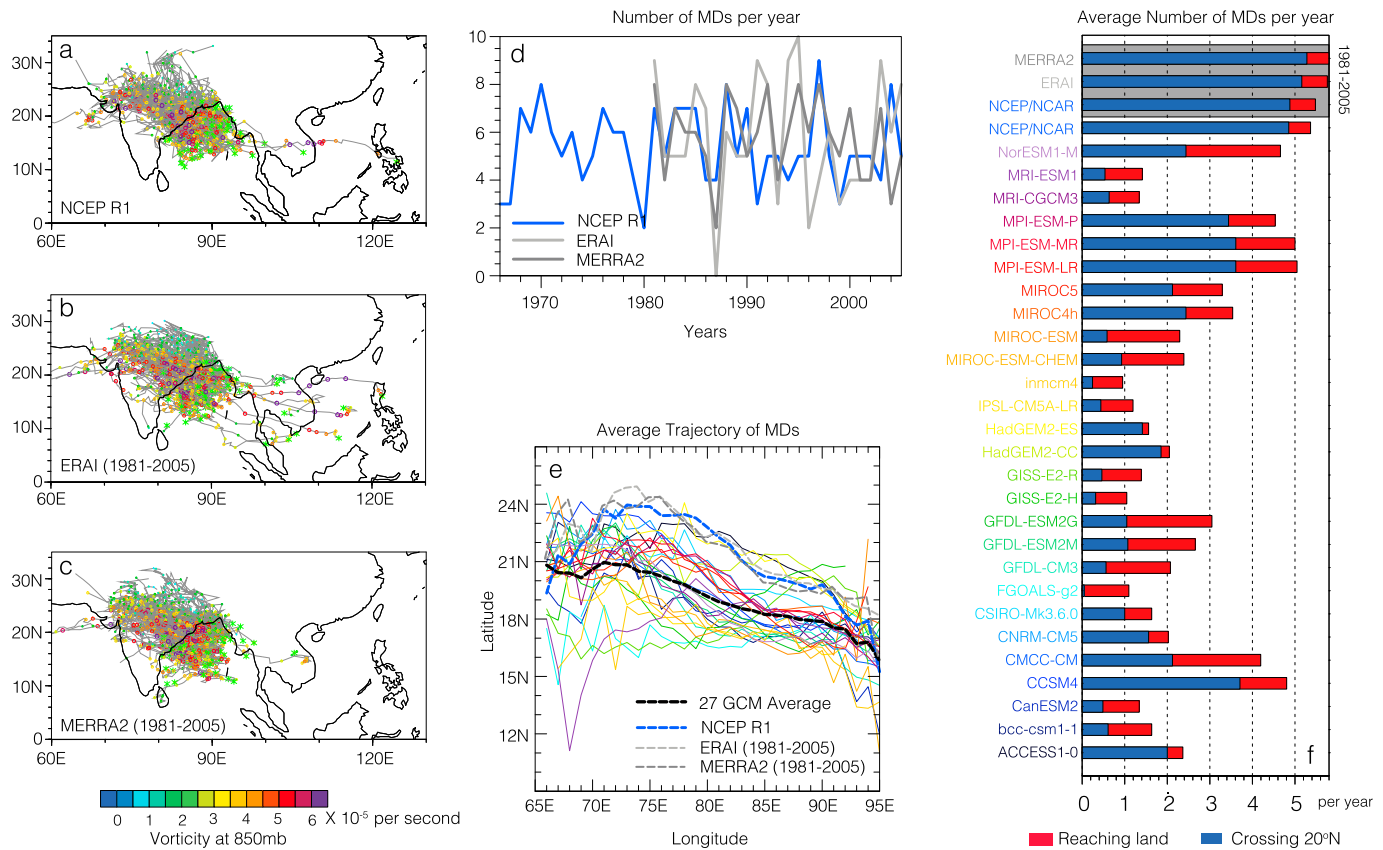


Figure 1. Characteristics of monsoon depressions (MDs) in the historical period. (a) Individual trajectories of MDs in National Centers for Environmental Prediction R1, (b) ERA-Interim, and (c) Modern-Era Retrospective analysis for Research and Applications 2. The green stars represent the starting point of each MD, and the colored circles represent the magnitude of relative vorticity every 12 hr. (d) Time series of number of MDs per year in Reanalysis data sets. (e) Mean trajectory of MDs in the Reanalysis and Coupled Model Intercomparison Project Phase 5 general circulation models (GCMs). (f) Number of MDs per year (red) and those that cross 20°N and move northwestward during their life span (blue). The color of each GCM name in (f) corresponds to the color of each line in (e). Historical period refers to 1965–2005 unless otherwise stated.

BoB and land originating MDs are considered over a bigger genesis domain (Praveen et al., 2015). Overall, MDs identified in NCEP R1, MERRA2, and ERA-I directly contributed more than 46% (45% when 1965–2005 is considered), 47%, and 37% precipitation to the total JJAS precipitation over the CI domain, respectively. GCMs in the CMIP5 models exhibit biases in the simulation of MD characteristics with on average, only 1 in 2 models simulating ~2 or more westward MDs per year and only 57% of those MDs follow trajectories north of 20°N over land (ranging from 5% to 90% in individual models with a mean standard deviation of $\pm 23\%$; Figures 1 and S2). A few GCMs, in particular FGOALS, also simulate eastward moving MDs, but such MDs are nonexistent in Reanalysis data sets (Figure S3). Therefore, any contribution coming from eastward moving MDs is ignored in our analyses. On average, MDs in the CMIP5 ensemble (Figure 1e, thick black dotted line) spend most of their lifecycle below 20°N while traveling from the BoB to central India, and they only travel across 20°N while traveling west of the CI domain. Since MDs provide a mechanism for moisture transport and wide spread precipitation over the land of South Asia, such biases in their trajectories will limit the amount of precipitation for the northern branch of the summer monsoon along the foothills of the Himalayas and parts of central India. Indeed, such underestimation of precipitation is reflected in the seasonal maps where models with at least 2 or more MDs per year tend to exhibit better skill in simulating the amount and spatial distribution of summer precipitation and the overlying lower level (850 mb) monsoon circulation (e.g., within the white square region; Figures 2a–2c). The linkage between the number of MDs and the amount of summer season precipitation has also been reported in previous studies (Praveen et al., 2015). The comparison of MDs and the precipitation distribution in the individual GCMs are provided in Figures S2 and S4. It should be noted that models that produce two or more MDs per year also tend to exhibit relatively better skill in their trajectories over land (Figures 1 and S2). Given the biases in the frequency and trajectories

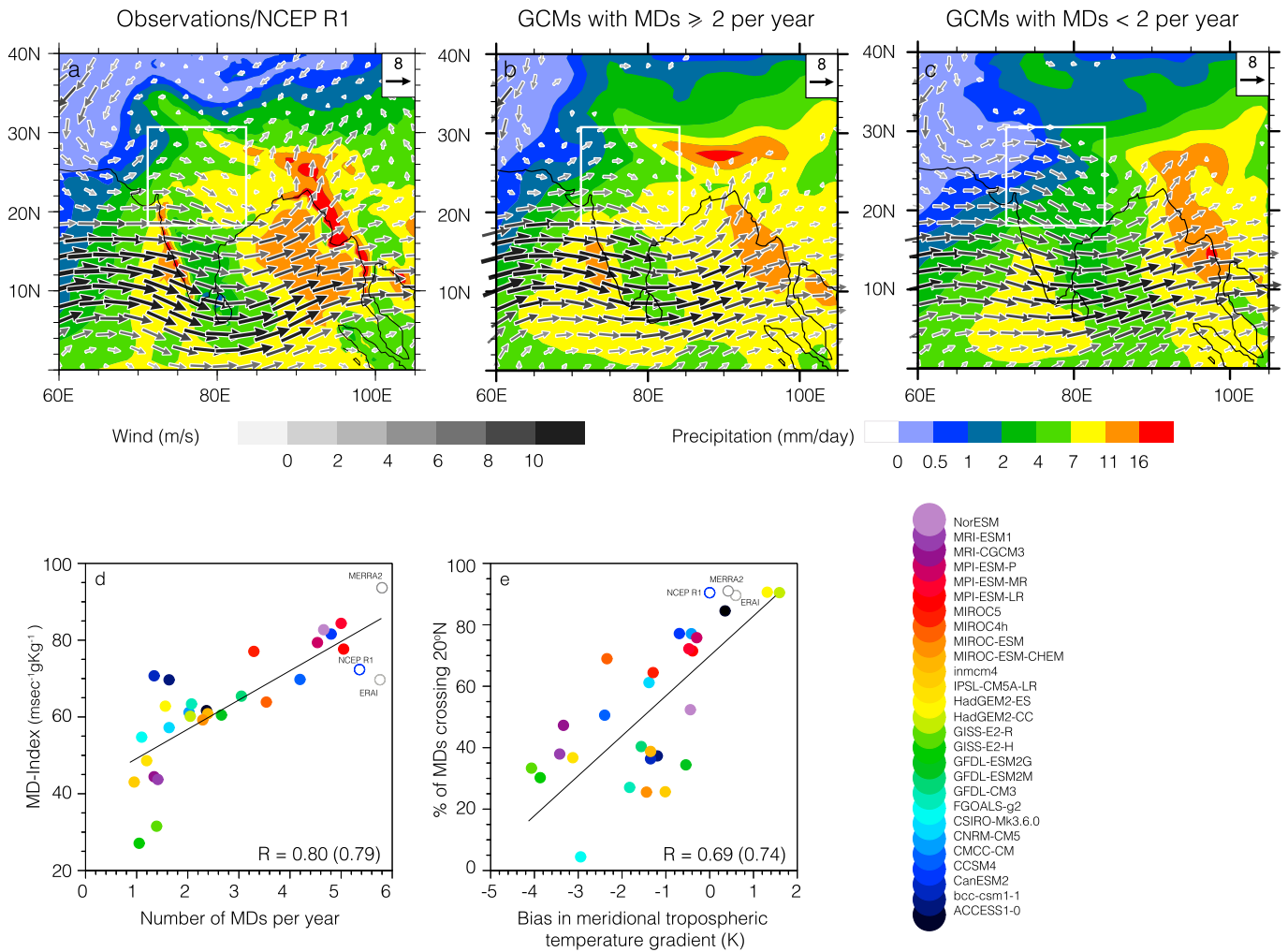


Figure 2. Historical period analyses. Summer monsoon precipitation (colored contours) and 850-hPa wind vectors in (a) observations/National Centers for Environmental Prediction R1, (b) general circulation models (GCMs) with at least two monsoon depressions (MDs) per year on average, and (c) GCMs with less than two MDs per year on average. Precipitation observations over land are from Climate Research Unit and over ocean are from Climate Prediction Center. The white square in Figures 2a to 2c provides a reference for comparison. (d) Number of MDs per year versus the MD-index. (e) Percent of MDs crossing 20°N versus bias in the meridional tropospheric temperature gradient is with respect to National Centers for Environmental Prediction R1. All analyses are based on 1965–2005 period except for ERA-Interim and Modern-Era Retrospective analysis for Research and Applications 2, which are based on 1981–2005. Correlations are based on GCMs (GCMs and Reanalysis data sets) in Figures 2d and 2e. The colors of individual GCMs in Figures 2d and 2e correspond to their colors in Figure 1.

of MDs, there is only a 27% (ranging from 6% to 50% in individual models with a mean standard deviation of $\pm 12\%$) contribution to the seasonal precipitation over the CI domain that comes directly from MDs in the ensemble mean of the CMIP5 GCMs.

The low-frequency bias of MDs in the historical experiments of the GCMs is associated with their poor simulation of a favorable background environment, indispensable for MD genesis. During the summer season, the mean southwesterly flow in the lower troposphere and the northeasterly flow in the upper troposphere provide the background relative vorticity field, which along with the moist background conditions over the core genesis region of MDs generate a suitable environment for the development of MDs. We combine these background conditions in an MD-index (see section 2) that exhibits 0.80 correlation with the mean frequency of MDs across the GCMs (correlation is 0.79 when both GCMs and Reanalysis are considered; Figure 2d).

On the other hand, errors in the simulation of MD trajectories over the land of South Asia are related to the biases in the MTG. A weak MTG in the GCMs tends to preclude the northwestward movement of MDs over

land (Figure 2e) by anomalously maintaining the monsoon trough south of its observed position. MDs move along the monsoon trough, which provides a background cyclonic vorticity through the convergence of southwesterly winds in its south and the northeasterly winds in its north. It has been shown previously (Ashfaq et al., 2016) that weaker than normal MTG in GCMs impacts the northward migration of monsoon trough during summer season and delays the northwestward progression of the monsoon onset. Our results indicate that such errors in the monsoon characteristics also push MDs in the west-southwestward direction south of 20°N (Figures 1c and 2e). When compared across the GCMs (or GCM and Reanalysis), a statistically significant relationship at the 99% confidence level exists between the simulated strength of the MTG and the average number of MDs that travel north of 20°N per year. Bias in the MTG in the CMIP5 GCMs is related to the errors in their simulated premonsoon diabatic heating that delays strengthening and seasonal reversal of the MTG (from negative to positive) and the monsoon onset over land. Late arrival of precipitation over land induces errors in the latent heat driven atmospheric heating, further exacerbating the bias in the MTG (Ashfaq et al., 2016).

3.2. MDs in the Future Period

Future trends in MDs are presented as the mean of the 20 models that have data available for the entire length of the analysis period (Table S1). MDs exhibit an insignificant decreasing trend in their yearly occurrences during the 21st century, which is predominantly driven by long-lived MDs (5 days or longer), as most of the MDs in the CMIP5 GCMs last for 5 days or longer (Figure 3a). The response in the case of short-lived MDs (>2days and <5 days) is relatively muted, which can also be due to their inherent low frequency in the models (Figure 3a). In addition to the long-term trend, difference in the future changes in the frequency of MDs between the first (2010–2054) and second (2055–2099) half of the 21st century for individual models also fails the significance test, so it cannot be concluded that there is a significant decline in the frequency of MDs. It should be noted that a recent study that makes use of a high-resolution atmosphere-only model driven by SSTs from CMIP5 GCMs also suggests a decline in the number and northward shift in the genesis of low-pressure systems (Sandeep et al., 2018).

A robust downward trend in the yearly occurrence of MDs during the 21st century is potentially lacking due to inconsistent changes in the background environment linked to the occurrences of MDs in the historical experiments of GCMs (Figure 2d). In the case of the ensemble mean of GCMs, a progressive weakening trend is exhibited in U_{850} and V_{200} , which is significant at the 99% significance level. However, as expected in a warmer climate, $Q_{850 \text{ to } 500}$ exhibits a strong increasing trend over the BoB (Figure 3b). While weaker dynamics tends to make background conditions unfavorable for the genesis of MDs, an increase in the lower-to-middle tropospheric moisture makes the condition more conducive for deep convection over the core region. These counteracting mechanisms lead to insignificant decreases in the MD frequency even at the higher levels of radiative forcing by the end of 21st century. It should be noted that the relationship between the strength of the MD-index and the mean frequency of MDs across the GCMs remains significant at the 99% level in the future period (Figure S5); however, increasingly moisture-driven monsoonal response weakens the strength of this relationship (for 20 GCMs) from 0.84 in the historical period to 0.73 in the first half (2010–2054) and to 0.68 in the second half (2055–2099) of the 21st century (Figure S5).

The lack of a robust trend in MDs and inconsistent changes in the background monsoon dynamics and atmospheric moisture across the GCMs is due to their equivocal responses. For instance, out of 20 GCMs in the future period, a significant trend is exhibited by only 3 (2 positive, 1 negative), 2 (1 positive, 1 negative), and 4 (3 positive, 1 negative) in 2010–2099, 2010–2055, and 2056–2099 periods, respectively (Table S2). Similarly, weakening of the background dynamics is not a robust response across the individual GCMs. While the median trend in both $|V_{200}|$ and $|U_{850}|$ reflects weakening, a number of models exhibit a strengthening trend particularly in the case of $|V_{200}|$ (Figure 3g). Likewise, GCMs do not exhibit robust changes in the characteristics of MDs such as duration, frequency, and total number of MD-days between the first and second half of the 21st century at various levels of the cumulative distribution function (Figure S6).

Additionally, little or no change is noted in the trajectories of MDs over the South Asian landmass in the future period (Figure 3c). This lack of change in the MDs trajectories over land contrasts with the robust weakening of MTG in the GCMs (Figure 3d), which is driven by warmer sea surface temperatures and stronger latent heating over the ocean (Ashfaq et al., 2009). Historical biases in the trajectories of MDs in GCMs can

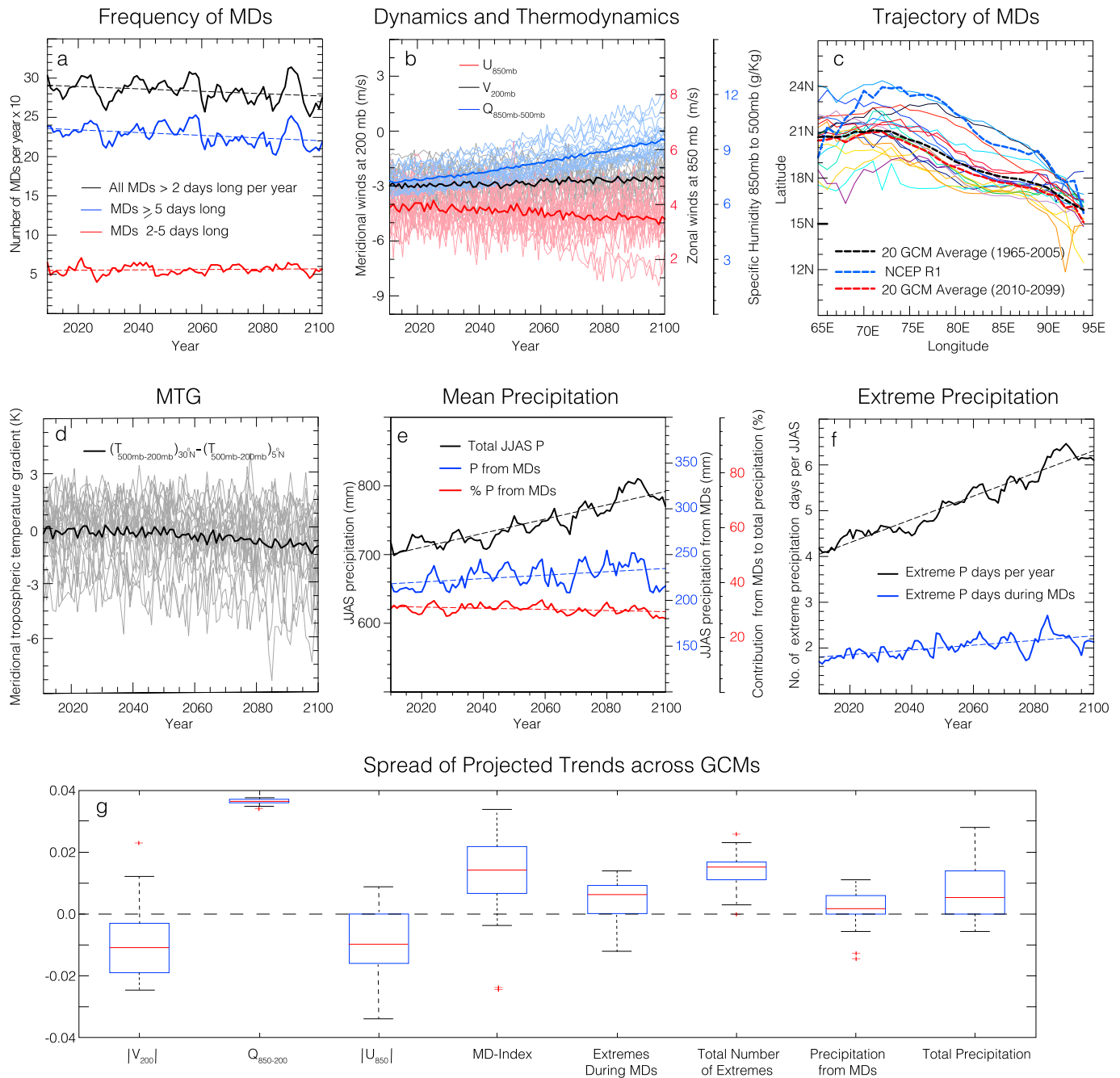


Figure 3. Future period (2010–2099) analyses. (a) Ensemble mean 5-year running mean of all monsoon depressions (MDs) with lifespan >2 days (black line), MDs with lifespan ≥ 5 days (blue), and MDs with lifespan >2 days and <5 days (red). (b) Time series of U_{850} (red), V_{200} (black), and $Q_{850-500}$ (blue). The thick lines represent ensemble mean, and the thin lines represent each of the 20 Coupled Model Intercomparison Project Phase 5 (CMIP5) general circulation models (GCMs). (c) Mean trajectory of MDs in National Centers for Environmental Prediction R1 in the historical period (dotted black), GCM ensemble mean in the historical period (dotted red), GCM ensemble mean in the future period (dotted blue), and each GCM in the future period (thin colored) over South Asia. The colors of the GCMs in Figure 3c correspond to their colors in Figure 1. (d) Time series of MTG in ensemble mean (black) and individual GCMs (thin gray). (e) Ensemble mean 5-year running mean of total summer precipitation (black), precipitation during MDs (blue), and % contribution from MDs to the total precipitation (red). (f) Number of wet extremes (>95th percentile of the historical period precipitation) per summer in the ensemble mean (black) and number of wet extremes during the life span of MDs (blue) per summer. (g) Box and whisker plots showing the spread of projected trends across CMIP5 GCMs for different normalized variables.

potentially be one of the factors contributing to this disconnect as most of the MDs in the historical experiment of the GCMs are already west-southwestward of their paths in Reanalysis and observations, so further weakening of the MTG has a limited influence on the paths taken by the MDs in the future period (Figure 2d). Additionally, the magnitude of the MTG weakening in the future period is much weaker than the magnitude of the MTG bias in the historical experiment of the GCMs, so a significant impact of future weakening of the MTG is not expected (Figures 2e and 3d).

3.3. Future Changes in the Characteristics of Precipitation

Driven by a slight decrease in the MDs, the percent contribution of MDs to the total summer precipitation exhibits a decreasing trend despite the fact that the absolute magnitude of precipitation from the MDs shows an upward trend (Figure 3e). Overall, there is a significant increasing trend in the summer precipitation (Figure 3e, black line) during the 21st century due to the moister atmospheric conditions (Figure 3b, green line). However, the increase in precipitation associated with the MDs is compensated for by a net decrease in the total number of days with an MD over land. Increasing trends in total precipitation and decreasing trend in percent contribution by the MDs to the total are significant at the 99% confidence level. Future increases in mean seasonal precipitation are influenced by the increase in the number of extreme precipitation days (Figure 3f, black line). If we consider extremes based on the 95th percentile threshold from the historical period, up until the middle 21st century, a major part of the increase in extremes are due to MDs as approximately every one in three extremes occurs on a day when an MD is present over land. After the middle 21st century, the number of precipitation extremes during the lifetime of MDs becomes more variable at decadal time scales with no major trend, in contrast to the precipitation extremes on nondepression days that almost double in number during the latter half of the 21st century (Figure 3f). Again, a slight increase in the number of extremes during depression days can be attributed to the moister atmosphere that should lead to more days when daily precipitation amount crosses the historical threshold (95th percentile) for extremes. The nature of changes in extremes is analogous when the 99th percentile of historical period precipitation is considered as threshold for defining daily precipitation extremes (not shown). Similarly, relatively robust increasing trends exist across the models for total precipitation and number of wet extremes, which is mostly lacking in the case of precipitation from MDs and the number of extremes during the MDs lifespan (Figure 3g).

4. Conclusions

Monsoon depressions over South Asia are a critical source of moisture transport and widespread precipitation across the region, particularly over the more inland parts of central and western South Asia. Current projections based on the CMIP5 GCMs suggest that there may not be a significant change in the frequency and trajectories of MDs in the 21st century under RCP8.5; however, these projections are partly overshadowed by the inherent inability of GCMs to produce as many MDs as those in the observations and to simulate their north-northwestward trajectories over land. This study does not make a distinction between MDs and low-pressure systems based on the wind speed. However, we do not expect significant changes in our conclusions with the application of further constraints on the selection of MDs in our analyses. This argument is partly supported by the findings of a recent study that suggests a decline in the number and northward shift in the genesis of low-pressure systems when results from a high-resolution atmosphere-only model, which makes use of SSTs from CMIP5 GCMs, are considered (Sandeep et al., 2018). While differences in the experimental design and analyses limit our ability to draw parallels between our findings and those of Sandeep et al. (2018), they highlight the need for better modeling strategies and more rigorous investigation of expected changes in the characteristics of MDs over South Asia.

Despite the lack of significant trends in MDs, there are important changes in the monsoon behavior at seasonal to daily time scales, particularly those related to mean and extreme precipitation. For instance, a significant increase in high-intensity precipitation events outside of the MD lifecycle heightens the unpredictable nature of monsoon extremes. Similarly, the increasingly moisture-driven future response warrants the enervation of any thermodynamically or dynamically driven downward trends in MDs that may currently exist in the observations, favoring the prevailing lack of trend reported in Reanalysis data sets.

Acknowledgments

We thank two anonymous reviewers for helpful and insightful comments. This work is supported by the Department of Energy Office of Science Biological and Environmental Research as part of the Regional and Global Climate Modeling program. Support for data storage and analysis is provided by the Oak Ridge Leadership Computing Facility at the Oak Ridge National Laboratory (ORNL), which is supported by the Office of Science of the U.S. Department of Energy (DOE) under contract DE-AC05-00OR22725. We thank U.S. DOE's Program for Climate Model Diagnosis and Intercomparison for providing coordinating support and leading development of software infrastructure in partnership with the Global Organization for Earth System Science Portals for CMIP. All westward moving MD data sets used in this study are part of the supporting information. Pacific Northwest National Laboratory is operated for DOE by Battelle Memorial Institute under contract DE-AC05-76RL01830.

References

- Annamalai, H., Hamilton, K., & Sperber, K. R. (2007). The South Asian summer monsoon and its relationship with ENSO in the IPCC AR4 simulations. *Journal of Climate*, 20(6), 1071–1092. <https://doi.org/10.1175/JCLI4035.1>
- Ashfaq, M., Rastogi, D., Mei, R., Touma, D., & Leung, L. R. (2016). Sources of errors in the simulation of south Asian summer monsoon in the CMIP5 GCMs. *Climate Dynamics*, 49(1–2), 193–223. <https://doi.org/10.1007/s00382-016-3337-7>
- Ashfaq, M., Shi, Y., Tung, W. W., Trapp, R. J., Gao, X. J., Pal, J. S., & Diffenbaugh, N. S. (2009). Suppression of south Asian summer monsoon precipitation in the 21st century. *Geophysical Research Letters*, 36, L01704. <https://doi.org/10.1029/2008gl036500>
- Boos, W. R., & Hurley, J. V. (2013). Thermodynamic bias in the multimodel mean boreal summer monsoon. *Journal of Climate*, 26(7), 2279–2287. <https://doi.org/10.1175/JCLI-D-12-00493.1>
- Cohen, N. Y., & Boos, W. R. (2014). Has the number of Indian summer monsoon depressions decreased over the last 30 years? *Geophysical Research Letters*, 41, 7846–7853. <https://doi.org/10.1002/2014gl061895>
- Dash, S. K., Kumar, J. R., & Shekhar, M. S. (2004). On the decreasing frequency of monsoon depressions over the Indian region. *Current Science India*, 86(10), 1404–1411.
- Dee, D. P., Uppala, S. M., Simmons, A. J., Berrisford, P., Poli, P., Kobayashi, S., et al. (2011). The ERA-Interim reanalysis: Configuration and performance of the data assimilation system. *Quarterly Journal of the Royal Meteorological Society*, 137(656), 553–597. <https://doi.org/10.1002/qj.828>
- Galarneau, T. J., Hamill, T. M., Dole, R. M., & Perlwitz, J. (2012). A multiscale analysis of the extreme weather events over western Russia and northern Pakistan during July 2010. *Monthly Weather Review*, 140(5), 1639–1664. <https://doi.org/10.1175/MWR-D-11-00191.1>
- Gelaro, R., McCarty, W., Suárez, M. J., Todling, R., Molod, A., Takacs, L., et al. (2017). The Modern-Era Retrospective Analysis for Research and Applications, version 2 (MERRA-2). *Journal of Climate*, 30(14), 5419–5454. <https://doi.org/10.1175/JCLI-D-16-0758.1>
- Goswami, B. N., Venugopal, V., Sengupta, D., Madhusoodanan, M. S., & Xavier, P. K. (2006). Increasing trend of extreme rain events over India in a warming environment. *Science*, 314(5804), 1442–1445. <https://doi.org/10.1126/science.1132027>
- Hagos, S., Leung, L. R., Zhao, C., Feng, Z., & Sakaguchi, K. (2018). How do microphysical processes influence large-scale precipitation variability and extremes? *Geophysical Research Letters*, 45, 1661–1667. <https://doi.org/10.1002/2017gl076375>
- Hamed, K. H., & Rao, A. R. (1998). A modified Mann-Kendall trend test for autocorrelated data. *Journal of Hydrology*, 204(1–4), 182–196. [https://doi.org/10.1016/S0022-1694\(97\)00125-X](https://doi.org/10.1016/S0022-1694(97)00125-X)
- Harris, I., Jones, P. D., Osborn, T. J., & Lister, D. H. (2014). Updated high-resolution grids of monthly climatic observations—The CRU TS3.10 Dataset. *International Journal of Climatology*, 34(3), 623–642. <https://doi.org/10.1002/joc.3711>
- Hodges, K. I. (1995). Feature tracking on the unit-sphere. *Monthly Weather Review*, 123(12), 3458–3465. [https://doi.org/10.1175/1520-0493\(1995\)123<3458:Ftotus>2.0.Co;2](https://doi.org/10.1175/1520-0493(1995)123<3458:Ftotus>2.0.Co;2)
- Hodges, K. I. (1999). Adaptive constraints for feature tracking. *Monthly Weather Review*, 127(6), 1362–1373. [https://doi.org/10.1175/1520-0493\(1999\)127<1362:Acfft>2.0.Co;2](https://doi.org/10.1175/1520-0493(1999)127<1362:Acfft>2.0.Co;2)
- Holloway, C. E., & Neelin, J. D. (2009). Moisture vertical structure, column water vapor, and tropical deep convection. *Journal of the Atmospheric Sciences*, 66(6), 1665–1683. <https://doi.org/10.1175/2008jas2806.1>
- Hunt, K. M. R., Turner, A. G., & Parker, D. E. (2016). The spatiotemporal structure of precipitation in Indian monsoon depressions. *Quarterly Journal of the Royal Meteorological Society*, 142(701), 3195–3210. <https://doi.org/10.1002/qj.2901>
- Hurley, J. V., & Boos, W. R. (2015). A global climatology of monsoon low-pressure systems. *Quarterly Journal of the Royal Meteorological Society*, 141(689), 1049–1064. <https://doi.org/10.1002/qj.2447>
- Kistler, R., Collins, W., Saha, S., White, G., Woollen, J., Kalnay, E., et al. (2001). The NCEP-NCAR 50-year reanalysis: Monthly means CD-ROM and documentation. *Bulletin of the American Meteorological Society*, 82(2), 247–267. [https://doi.org/10.1175/15200477\(2001\)082<0247:Tnnyrm>2.3.Co;2](https://doi.org/10.1175/15200477(2001)082<0247:Tnnyrm>2.3.Co;2)
- Mei, R., Ashfaq, M., Rastogi, D., Leung, L. R., & Dominguez, F. (2015). Dominating controls for wetter South Asian Summer Monsoon in the Twenty-First Century. *Journal of Climate*, 28(8), 3400–3419. <https://doi.org/10.1175/JCLI-D-14-00355.1>
- Prajeesh, A. G., Ashok, K., & Rao, D. V. B. (2013). Falling monsoon depression frequency: A Gray-Sikka conditions perspective. *Scientific Reports-UK*, 3, 2989. <https://doi.org/10.1038/srep02989>
- Praveen, V., Sandeep, S., & Ajayamohan, R. S. (2015). On the relationship between mean monsoon precipitation and low pressure systems in climate model simulations. *Journal of Climate*, 28(13), 5305–5324. <https://doi.org/10.1175/JCLI-D-14-00415.1>
- Ramesh, K. V., & Goswami, P. (2014). Assessing reliability of regional climate projections: The case of Indian monsoon. *Scientific Reports-UK*, 4, 4071. <https://doi.org/10.1038/srep04071>
- Rao, B. R. S., Rao, D. V. B., & Rao, V. B. (2004). Decreasing trend in the strength of tropical easterly jet during the Asian summer monsoon season and the number of tropical cyclonic systems over Bay of Bengal. *Geophysical Research Letters*, 31, L14103. <https://doi.org/10.1029/2004gl019817>
- Sandeep, S., Ajayamohan, R. S., Boos, W. R., Sabin, T. P., & Praveen, V. (2018). Decline and poleward shift in Indian summer monsoon synoptic activity in a warming climate. *Proceedings of the National Academy of Sciences of the United States of America*, 115(11), 2681–2686. <https://doi.org/10.1073/pnas.1709031115>
- Sharjeel, S., Al-Arief, M., & Khan, M. I. (2012). ADB-WB assess Pakistan flood damage at \$9.7 billion, edited, World Bank.
- Sikka, D. R. (1977). Some aspects of life-history, structure and movement of monsoon depressions. *Pure and Applied Geophysics*, 115(5–6), 1501–1529. <https://doi.org/10.1007/Bf00874421>
- Singh, D., Horton, D. E., Tsiang, M., Haugen, M., Ashfaq, M., Mei, R., et al. (2014). Severe precipitation in northern India in June 2013: Causes, historical context, and changes in probability. *Bulletin of the American Meteorological Society*, 95(9), S58–S61.
- Soden, B. J., & Fu, R. (1995). A satellite analysis of deep convection, upper-tropospheric humidity, and the greenhouse-effect. *Journal of Climate*, 8(10), 2333–2351. [https://doi.org/10.1175/1520-0442\(1995\)008<2333:Asaodc>2.0.Co;2](https://doi.org/10.1175/1520-0442(1995)008<2333:Asaodc>2.0.Co;2)
- Sperber, K., Annamalai, H., Kang, I. S., Kitoh, A., Moise, A., Turner, A., et al. (2013). The Asian summer monsoon: An intercomparison of CMIP5 vs. CMIP3 simulations of the late 20th century. *Climate Dynamics*, 41(9–10), 2711–2744. <https://doi.org/10.1007/s00382-012-1607-6>
- Vishnu, S., Francis, P. A., Shenoi, S. S. C., & Ramakrishna, S. S. V. S. (2016). On the decreasing trend of the number of monsoon depressions in the Bay of Bengal. *Environmental Research Letters*, 11(1), 014011. <https://doi.org/10.1088/1748-9326/11/1/014011>
- Xie, P. P., Janowiak, J. E., Arkin, P. A., Adler, R., Gruber, A., Ferraro, R., et al. (2003). GPCP pentad precipitation analyses: An experimental dataset based on gauge observations and satellite estimates. *Journal of Climate*, 16(13), 2197–2214. <https://doi.org/10.1175/2769.1>